www.czasopisma.pan.pl PAN POLSKA AKADEMIA NAUK www.journals.pan.pl

A R C H I V E S O F M E T A L L U R G Y A N D M A T E R I A L S

Volume 59 2014 Issue 1

DOI: 10.2478/amm-2014-0043

M. NABIAŁEK*, A. DOBRZAŃSKA-DANIKIEWICZ**, S. LESZ**, P. PIETRUSIEWICZ*, M. SZOTA***, M. DOŚPIAŁ*

EFFECT OF COOLING RATE ON MAGNETIC PROPERTIES, SIZE AND TYPE OF STRUCTURAL DEFECTS IN THE VOLUME OF BULK AMORPHOUS $Fe_{36}Co_{36}B_{19}Si_5Nb_4$ ALLOY IN THE FORM OF RODS OF VARIOUS DIAMETERS

WPŁYW PRĘDKOŚCI CHŁODZENIA NA WŁAŚCIWOŚCI MAGNETYCZNE, WIELKOŚĆ I RODZAJ DEFEKTÓW STRUKTURALNYCH W STOPIE AMORFICZNYM $Fe_{36}Co_{36}B_{19}Si_5Nb_4$ W POSTACI PRĘTÓW O RÓŻNYCH ŚREDNICACH

This paper presents the results of microstructure and magnetic properties analysis for bulk amorphous samples of $Fe_{36}Co_{36}B_{19}Si_5Nb_4$ alloy in the form of rods of 1 mm, 2 mm, and 3 mm diameters in the as-cast state, produced using the method of injecting liquid alloy into cooled copper mold. The main purpose of the research was to examine the effect of solidification speed of the liquid material into amorphous state on the shape of initial magnetization curve as well as to determine the type and size of structural defects occurring in the volume of the material. In order to achieve these objectives, the magnetization measurements were carried out, which according to H. Kronmüller's theory on magnetization behavior near the area called reaching the ferromagnetic saturation, allow to determine the type, size, and surface density of structural defects occurring in the volume of the sample. The analysis of reduced magnetization curves indicates that solidification speed of the liquid alloy into the amorphous state is the main determining factor for the shape of initial magnetization curve and for the type and size of structural defects formed in the sample, which affects such magnetic parameters as: coercive field (H_C) or saturation magnetization (M_S).

Keywords: bulk amorphous alloy, point defects, quasi-dislocalized dipoles

W pracy przedstawiono wyniki badań mikrostruktury oraz właściwości magnetycznych masywnego stopu amorficznego $Fe_{36}Co_{36}B_{19}Si_5Nb_4$ w stanie po zestaleniu. Próbki stopu zostały wytworzone w postaci prętów o średnicy 1 mm, 2 mm i 3 mm przy zastosowaniu metody wtłaczania ciekłego materiału do miedzianej formy chłodzonej wodą. Mikrostrukturę próbek w stanie po zestaleniu badano wykorzystując dyfrakcję promieni Röntgena, natomiast magnetyzację w silnych polach magnetycznych mierzono wykorzystując magnetometr wibracyjny (VSM).

Głównym celem pracy było zbadanie wpływu czasu zestalania ciekłego materiału do stałego stanu amorficznego na przebieg pierwotnej krzywej magnesowania oraz określenie rodzaju i wielkości defektów strukturalnych występujących w badanych próbkach.

1. Introduction

Bulk amorphous alloys constitute a relatively new group of materials with very interesting magnetic and mechanical properties which are not observed in crystalline materials of the same chemical composition [1-10]. Those materials are characterized by high hardness, elasticity, wear and corrosion resistance, and excellent energy absorption ratio. Alloys based on 3d transition metals usually demonstrate good soft magnetic properties, i.e. small coercive field, and relatively high magnetic permeability and saturation magnetization. The shape of initial magnetization curves for those materials varies, depending on the alloy composition and thickness. According to H. Kronmüller's theory, the magnetization process in strong magnetic fields is affected by structural defects [11-12]. In high magnetic fields, above anisotropy field ($H > 2K_1/\mu_0 M_s$ where K_1 – effective anisotropy constant), a material losses its domain structure and is not yet uniformly magnetized. Magnetization of the sample does not reach the maximum value, called saturation magnetization, which is particularly affected by structural defects, i.e. point defects and quasi-dislocalized dipoles. Inside the material those defects make a source of short-range stresses and cause nonuniform magnetization distribution in microareas – Fig. 1.

The change in magnetization caused by structural defects can be described with a formula [11]:

$$\Delta M_{def} = \sum_i \frac{M_s a_i}{(\mu_0 H)^i}, \tag{1}$$

where: exponent (i) takes on three values of $^1/_2$, 1 and 2, M_s – saturation magnetization, H – magnetic field strength, μ_0 – vacuum magnetic permeability.

* INSTITUTE OF PHYSICS, CZĘSTOCHOWA UNIVERSITY OF TECHNOLOGY, 19 ARMII KRAJOWEJ AV., 42-200 CZĘSTOCHOWA, POLAND
** INSTITUTE OF ENGINEERING AND BIOMATERIALS, SILESIAN UNIVERSITY OF TECHNOLOGY, 18A KONARSKIEGO AV, 44-100 GLIWICE, POLAND
*** INSTITUTE OF MATERIAL SCIENCE, 19 ARMII KRAJOWEJ AV., 42-200 CZĘSTOCHOWA, POLAND

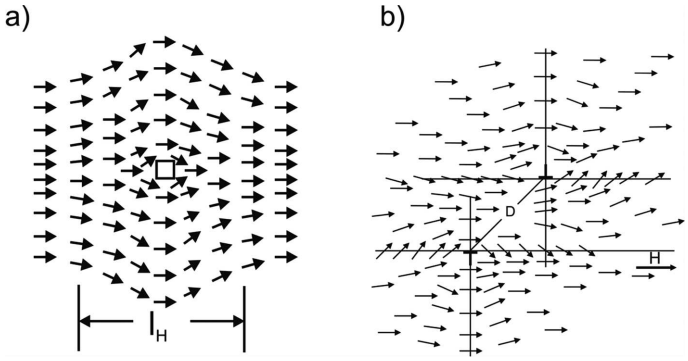

Fig. 1. (a) Magnetization distribution around a point defect, (b) Magnetization distribution around a quasi-dislocalized dipoles [11]

The exponent (i) takes on value of ($^1/_2$) for point defects and this expression can be presented with a formula (2) [12]:

$$\frac{a_{1/2}}{(\mu_0 H)^{1/2}} = \mu_0 \frac{3}{20A_{ex}} \left(\frac{1+\upsilon_p}{1-\upsilon_p}\right)^2 \times \\ \times G^2 \lambda_S^2 (\Delta V)^2 N \left(\frac{2A_{ex}}{\mu_0 M_s}\right)^{1/2} \times \frac{1}{(\mu_0 H)^{1/2}}, \tag{2}$$

where: A_{ex} – exchange constant, υ_p – Poisson's ratio, G – shear modulus, λ_S – saturation magnetostriction, N – defects density, ΔV – additional volume related to point defects.

For (i) = 1 or 2 the expression (1) takes on values of a_1 (3) and a_2 (4), which are assigned to the presence of two-dimensional defects, called quasi-dislocalized dipoles.

$$\frac{a_1}{(\mu_0 H)^1}, \tag{3}$$

$$\frac{a_2}{(\mu_0 H)^2}. \tag{4}$$

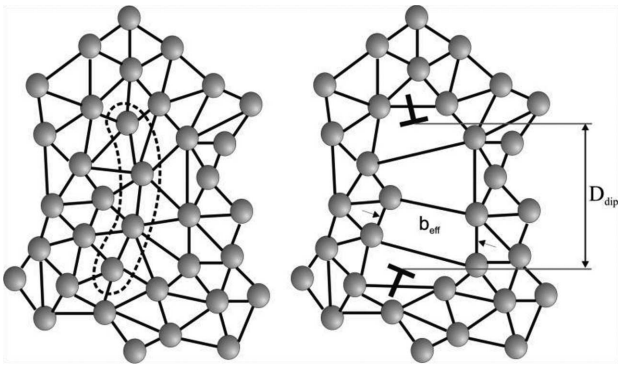

Fig. 2. Model of a quasi-dislocalized dipoles: b_{eff} – length of effective Burgers vector, D_{dip} – width of quasi-dislocalized dipoles [11, 12]

Linear defects are defined by: dipole width (D_{dip}), effective Burgers vector (b_{ef}) and defects surface density (N_p). If the exchange distance l_H^{-1}, described with a formula (5) [13]:

$$l_H^{-1} = \sqrt{\frac{2A_{ex}}{\mu_0 H M_S}}, \tag{5}$$

is greater than the width of quasi-dislocalized dipoles (D_{dip}) then the term (3) is dominant and can be described with a dependence (6) [14]:

$$\frac{a_1}{\mu_0 H} = 1,1\mu_0 \frac{G^2 \lambda_S^2}{\left(1-\upsilon_p\right)^2} \frac{N_p b_{ef}^2}{M_S A_{ex}} D_{dip}^2 \frac{1}{\mu_0 H}, \tag{6}$$

whereas if $l_H^{-1} < D_{dip}$ then the magnetization change in strong magnetic fields near the area called the "knee" is related to the expression (7) [14]:

$$\frac{a_2}{(\mu_0 H)^2} = 0,456\mu_0 \frac{G^2 \lambda_S^2}{\left(1-\upsilon_p\right)^2} \frac{N_p b_{ef}^2}{M_S^2} D_{dip}^2 \frac{1}{(\mu_0 H)^2}. \tag{7}$$

The model of a quasi-dislocalized dipoles is presented on Fig. 2.

In higher magnetic fields where dependencies (1), (2) and (3) are not met, the magnetization vector turn is caused by the damping of thermally excited spin waves. This phenomenon is called the Holstein-Primakoff paraprocess, and is described with a formula (8) [15]:

$$\Delta M_{sp} = b\,(\mu_0 H)^{1/2}, \tag{8}$$

where: b is a coefficient determined on the basis of spin waves theory and described with a formula (9) [16]:

$$b = 3.54 g \mu_0 \mu_B (1/4\pi D_{sp})^{3/2} kT (g\mu_B)^{1/2}, \tag{9}$$

where: k – Boltzman constant, μ_B – Bohr magneton, g – Landé g-factor, D_{sp} – stiffness of spin wave parameter.

The stiffness of spin wave parameter D_{sp} is directly related to the exchange constant A_{ex}, which is described with a formula (10) [17]:

$$A_{ex} = \frac{M_S D_{sp}}{2g\mu_B}. \tag{10}$$

Finally, the magnetization in strong magnetic field, when reaching the state of ferromagnetic saturation, can be presented with a dependence (11):

$$M(H) = M_S \left[1 - \frac{a_{1/2}}{(\mu_0 H)^{1/2}} - \frac{a_1}{(\mu_0 H)^1} - \frac{a_2}{(\mu_0 H)^2}\right] + b(\mu_0 H)^{1/2} + \chi H. \tag{11}$$

The purpose of this paper is to prove that the change in shape of initial magnetization curve for samples of $Fe_{36}Co_{36}B_{19}Si_5Nb_4$ alloy made by injection molding, is related to the cooling rate of the alloy during its solidification in the copper mold. To accomplish the purpose of the research, measurements of magnetization in strong magnetic fields were performed. They constituted a basis for the determination of the type, size and surface density of structural defects.

2. Experiment

The research material, in form of $Fe_{36}Co_{36}B_{19}Si_5Nb_4$ alloy, was obtained using components of following purity: Fe – 99.99%; Co – 99.99%; Nb – 99.999%, Si – 99.99%, B – 99.99%. Crystalline ingots of the alloy were remelted several times in order to properly mix the elements constituting the material. Bulk amorphous samples were made using the technique of injecting liquid material into cooled copper mold. Samples produced that way were shaped into rods of diameters of 1 mm, 2 mm, 3 mm and length of about 20 mm.

The microstructure of casted samples in post-solidification state was examined using XRD 7 X-ray diffractometer,

manufactured by Seifert-FPM. The diffraction of X-rays was performed using the cobalt radiation source with characteristic radiation CuK_α (1.54056 Å). Samples were scanned in range of angle 2 Θ from 30° to 80° with 0.02° resolution and 3 s irradiation time per step.

Static hysteresis loops and initial magnetization curves were measured using vibrating sample magnetometer VSM, manufactured by LakeShore, operating in the field up to 2 T.

The measurements of microstructure and magnetic properties, were carried out in room temperature. XRD studies were made on powdered samples obtained in low-energy conditions, which in case of structure research gave information on the whole material volume. The magnetic properties were done for samples in the form of rods with different diameters and same length. The magnetic measurements were corrected using the demagnetization factor resulting from the presence of magneto-static fields, related to the shape of the sample.4

3. Results

Fig. 3 presents X-ray diffraction patterns obtained for casted $Fe_{36}Co_{36}B_{19}Si_5Nb_4$ alloy samples in the form of rods of 1 mm, 2 mm and 3 mm diameters in the as-cast state.

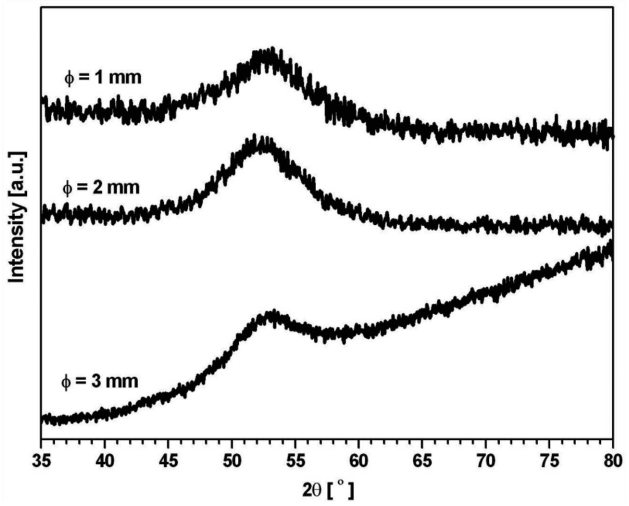

Fig. 3. Diffraction patterns obtained for samples of examined $Fe_{36}Co_{36}B_{19}Si_5Nb_4$ alloy in the as-cast state in the form of rods of 1 mm, 2 mm and 3 mm diameters

All diffraction patterns obtained for powdered rods of examined alloys are similar, they consist only of wide fuzzy maximums, which evidences the lack of crystallites in the entire volume of examined samples. Crystalline materials demonstrate repeated distribution of atoms in space, which maintain their angle correlations. It means that for crystalline materials it is possible to determine interplanar distances, which are reflected by narrow maximums in diffraction images. The lack of narrow maximums in X-ray diffractograms provides us with preliminary information about chaotic aperiodic distribution of atoms in examined material volume, which suggests that the examined material has an amorphous structure.

Static hysteresis loops obtained from measurements of magnetization in the function of magnetization field for samples of examined alloys in post-solidification state in the form of rods of various diameters are presented in Fig. 4.

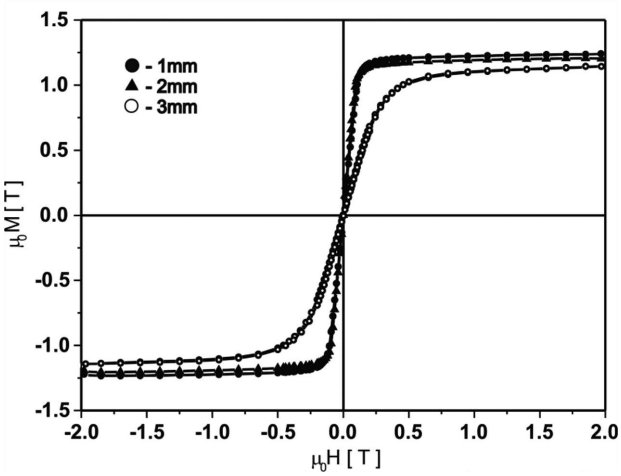

Fig. 4. Static hysteresis loops measured for samples of $Fe_{36}Co_{36}B_{19}Si_5Nb_4$ alloy in the form of rods of 1 mm, 2 mm, and 3 mm diameters in the as-cast state

The course of static hysteresis loops presented in Fig. 4 for 1 mm and 2 mm diameters rods is practically the same. We can observe that in the middle section of M-H system those loops are almost parallel to $\mu_0 M_S$ axis, which proves that both examined samples in the form of above diameters are rather easy to magnetize towards saturation, using magnetic fields of low strength. M-H dependence pattern for bulk 3 mm diameter sample is completely different from other examined samples. Its analysis indicates that the greatest diameter sample demonstrated "the worst" soft magnetic properties. Properties such as: coercive field (H_C) and saturation magnetization ($\mu_0 M$), determined with the observation of static hysteresis loops were presented in Tab. 1.

TABLE 1
Magnetic properties of the bulk amorphous $Fe_{36}Co_{36}B_{19}Si_5Nb_4$ rods

Diameter	Magnetic properties	
[mm]	M_s, [T]	H_c, [A/m]
1	1.24	20.7
2	1.21	55.7
3	1.18	79.6

Based on the data from Tab. 1 it can be concluded that with increasing diameter of rod with amorphous structure, in the volume of this material we observe changes in the distribution of atoms of elements included in the material. It causes the deterioration of soft magnetic properties for those materials. Reduced curves of initial magnetization for examined alloy in the form of rods of various diameters are presented in Fig. 5.

Reduced curves of initial magnetization for samples of examined 1 mm and 2 mm diameters alloy, presented in Fig. 5, overlap in the wide range of magnetic fields. It can suggest that for both samples magnetization process in strong magnetic fields follow the same law and reaches the ferromagnetic saturation in similar ranges of magnetization field strength. The analysis of reduced curves of magnetization in high magnetic fields for samples of examined alloy in the form of rods in the as-cast state indicates that in magnetization fields range of

0.21 T to 0.30 T for 1 mm diameter sample (Fig. 6) and in magnetization fields range of 0.21 T to 0.54 T for 3 mm diameter rod (Fig. 7) the reduced magnetization M/M_S becomes the linear function of $(\mu_0 H)^{-1}$.

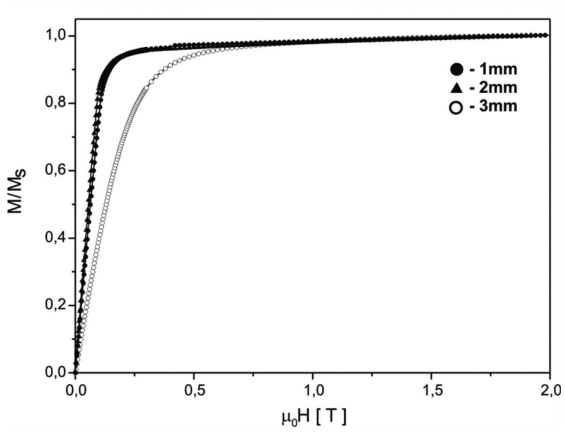

Fig. 5. Reduced magnetization curves for samples of amorphous $Fe_{36}Co_{36}B_{19}Si_5Nb_4$ alloy in the form of rods of 1 mm, 2 mm, and 3 mm diameters

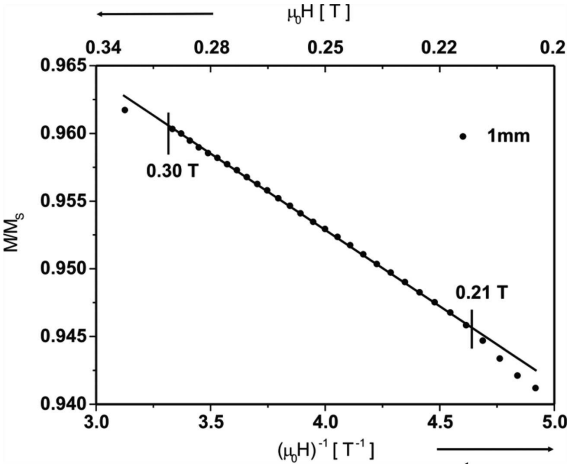

Fig. 6. Reduced magnetization curve $M/M_S = f[(\mu_0 H)^{-1}]$ measured for rod of 1 mm diameter

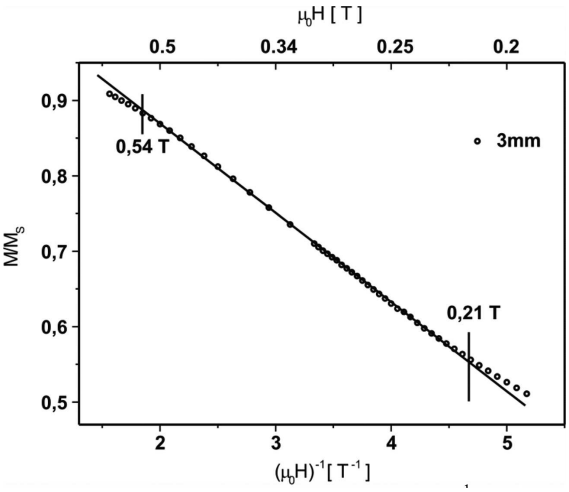

Fig. 7. Reduced magnetization curve $M/M_S = f[(\mu_0 H)^{-1}]$ measured for rod of 3 mm diameter

Such nature of magnetization changes, both for 1 mm and 3 mm diameter samples, proves that the magnetization process in this range of magnetic fields is related to the rotations of the magnetic moments inside structural defects, called quasi-dislocalized dipoles (Fig. 1b), with the dependence $D_{dip}l_H^{-1} < 1$ (where D_{dip} – width of quasi-dislocalized dipoles, l_H^{-1} – exchange distance).

For samples in the form of rods of 2 mm diameter in the magnetic fields range of 0.11 T to 0.31 T the reduced magnetization M/M_S is a linear function of $(\mu_0 H)^{-2}$, which also means that the magnetization process for this material in higher magnetic fields is related to the presence of quasi-dislocalized dipoles, but in this case the dependence $D_{dip}l_H^{-1} > 1$ holds (Fig. 8).

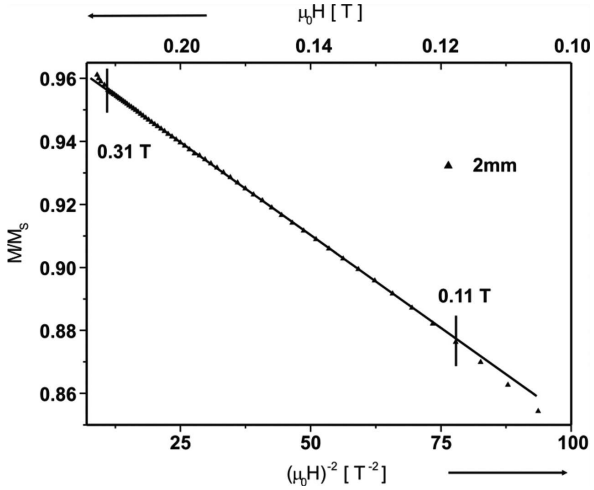

Fig. 8. Reduced magnetization curve $M/M_S = f[(\mu_0 H)^{-2}]$ measured for rod of 2 mm diameter

For higher values of magnetic field, from 0.3 T for 1 mm diameter rod, from 0.31 T for 2 mm diameter rod and from 0.54 T for 3 mm diameter rod of examined $Fe_{36}Co_{36}B_{19}Si_5Nb_4$ alloy, the Holstein-Primakoff paraprocess was observed (Fig. 9) [15].

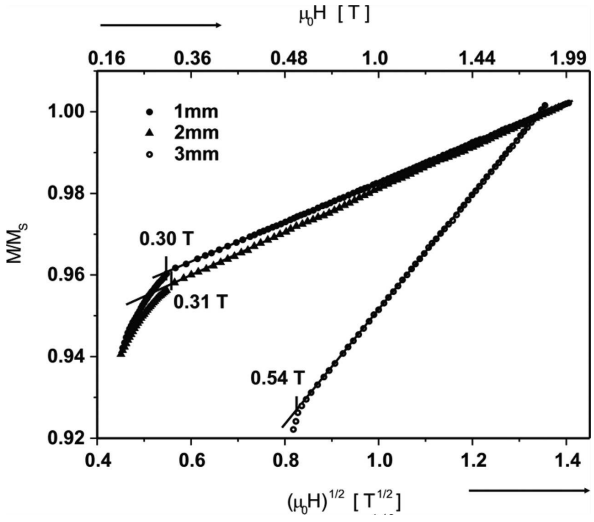

Fig. 9. Magnetization curves $M/M_S = f[(\mu_0 H)^{1/2}]$ determined for all examined samples

Tab. 2 presents results from the analysis of reduced magnetization as a function of magnetic field in powers of: -1, -2 and $^1/_2$.

TABLE 2

Data obtained from the analysis of reduced magnetization as a function of magnetic field strength in powers of: -1, -2 and $^1/_2$. The parameters a_1, a_2, b are the fit parameters of reduced magnetization as functions of $(\mu_0 H)^{-1}$, $(\mu_0 H)^{-2}$, $(\mu_0 H)^{1/2}$, respectively: D_{sp} – stiffness of spin wave parameter, A_{ex} – exchange constant, D_{dip} – width of quasi-dislocalized dipoles, and N – surface density of quasi-dislocalized dipoles

$Fe_{36}Co_{36}B_{19}Si_5Nb_4$ in the as – quenched state							
Diameter of sample [mm]	**a_1 [10^{-2} T]**	**a_2 [10^{-3} T^2]**	**b [10^{-2} $T^{1/2}$]**	**A_{ex} [10^{-11} Jm^{-1}]**	**D_{sp} [10^{-2} meVnm^2]**	**D_{dip} [10^{-9} m]**	**N [10^{16} m^{-2}]**
1	1.11		4.84	2.03	50.04	4.59	4.74
2	–	1.18	5.25	1.88	47.37	4.29	5.43
3	11.85		14.05	0.97	24.59	2.31	18.70

The data collected in Tab. 2 indicates that the surface density of structural defects present in samples is highest for the sample in the form of 3 mm diameter rod. For other samples of examined $Fe_{36}Co_{36}B_{19}Si_5Nb_4$ alloy in the form of 1 mm and 2 mm diameters rods the surface density of quasi-dislocalized dipoles present in the whole volume of examined material is similar.

4. Discussion of the results

The production of amorphous materials through rapid cooling brings about a significant number of structural defects, in the form of point defects, called free volumes, or in the form of quasi-dislocalized dipoles, which are conglomerates of point defects. Those defects are defined as excessive volume and form a source of internal mechanical stresses, which is reflected by a nonuniform distribution of magnetic moments, caused by magnetoelastic effects.

This research included the examination of magnetization in strong magnetic fields with so called reaching the ferromagnetic saturation. The authors also attempted to explain dependencies between the cooling time of the material, its magnetic properties, and the presence of structural defects in its volume. The X-ray examination carried out in the course of the research indicate that the samples produced using the injection molding are not crystalline. Based on the analysis of reduced magnetization in functions $(\mu_0 H)^{-1}$ and $(\mu_0 H)^{-2}$ for samples of examined alloy of various diameters, it was found out that the greatest the diameter of casted rods, the greater the surface density of structural defects in the form of quasi-dislocalized dipoles. It should be noted that all examined samples were made in identical conditions, i.e. the atmosphere of alloy injection, the temperature of copper mold, and the pressure of liquid material injection. Interestingly, a dependence $M/M_S = f[(\mu_0 H)^{-1}]$ holds for 1 mm and 3 mm diameters samples, while for 2 mm diameter sample another dependence $M/M_S = f[(\mu_0 H)^{-2}]$ was observed. The question is, what happens to the atoms during the cooling process? Most probably, increased time of liquid metal solidification into the amorphous state has an relaxing effect on the alloy. The result is a good elastic recovery of the alloy. During this process free volumes form greater two-dimensional defects through conglomeration, after reaching certain critical size those defects, due to a lack of stability, start to change their size and finally decompose into point defects again. Further increase of rods diameter, causing the increase of cooling time, would lead to the formation of crystalline phase grains, and subsequently to the full crystallization of the material.

Experiment results obtained from magnetization measurements in strong magnetic fields for samples of $Fe_{36}Co_{36}B_{19}Si_5Nb_4$ alloy in the form of rods of various diameters: 1 mm, 2 mm, and 3 mm, allowed to determine proper matching of laws of reaching the ferromagnetic saturation. The best matching was obtained for samples of 1 mm and 3 mm diameters:

$$M(H) = M_S\left[1 - \frac{a_1}{(\mu_0 H)^1}\right] + b(\mu_0 H)^{1/2}, \tag{12}$$

while for 2 mm diameter rod the best matching was obtained for the dependence:

$$M(H) = M_S\left[1 - \frac{a_2}{(\mu_0 H)^2}\right] + b(\mu_0 H)^{1/2}. \tag{13}$$

The parameter a_1 was found for higher magnetic fields from the range of 0.21 T< μ_0H <0.30 T and 0.21 T< μ_0H <0.54 T for rods of 1mm and 3 mm diameters, respectively, while the parameter a_2 for 2 mm diameter sample, where the best matching of the law of reaching the ferromagnetic saturation was obtained in the magnetic field range of 0.11 T< μ_0H <0.31 T. Observed dependencies are directly related to the change of exchange distance (A_{ex}), in the way defined by (6) and (7).

The application of the formula (9) allows to determine the stiffness of spin wave parameter D_{sp} in room temperature. Values calculated for D_{sp} fall into the range of 25 to 50 (10^{-2} meVnm^2). For amorphous alloys, all values from this range are acceptable, due to a lack of magnetocrystalline anisotropy of significant values [16]. When decreasing the D_{sp} parameter there occurs the increase of surface density N, which means that the distance between the nearest-neighbor atoms decreases in the volume of the material. It should be added, that publications [18, 19], which present research results for alloys of chemical composition which is slightly different from the ones examined in this paper, show that (Fe, Co) and B materials include trigonal bonds between atoms of Co or Fe and B. In case of this research those could be separated from each other and through the wall surface by Nb, acting as a binding agent for the atoms. The presence of those bonds cause the occurrence of initial crystallization fcc phase $(Fe, Co)_{23}B_6$ with lattice spacing of 1.2 nm and cubic cell of 96 atoms per volume unit. It means that the existence of

such systems with short-range order (SRO) can affect their displacement in the alloy during diffusion processes leading to temporary solidification of vitreous state (SL). It was not possible to evidence the existence of fcc phase in examined samples in the form of rods of various diameters during the X-ray examination carried out in this research.

This research allows to state that the increase in the diameter of casted rod of examined alloy leads to the worsening of so called soft magnetic properties of this material. It is also obvious that for a greater diameter rod the solidification takes longer in comparison to the solidification of smaller diameter sample, thus the diffusion process also takes longer and leads to more intensive displacement of atoms. Atoms migration in the alloy volume causes the extensive volumes formation, which, depending on the amorphous state solidification time, group into greater structural defects called quasi-dislocalized dipoles, and in longer term decompose into point defects again. The type of structural defects for examined samples, determined in the course of research, which could be examined with a indirect method of analyzing the reduced saturation magnetization near the "knee" area, affects the change of exchange distances for ferromagnetic effects between Fe and Co magnetic atoms.

REFERENCES

[1] K.Q. Qiu, H.F. Zhang, A.M. Wang, B.Z. Ding, Z.Q. Hu, Glass-forming ability and thermal stability of $Nd_{70-x}Fe_{20}Al_{10}Y_x$ alloys, Acta Mater. **50**, 3567-3578 (2002).

[2] M. Nabialek, M. Dospial, M. Szota, J. Olszewski, S. Walters, Manufacturing of the bulk amorphous $Fe_{61}Co_{10}Zr_{2+x}Hf_{3-x}W_2Y_2B_{20}$ alloys (where x = 1, 2, 3) their microstructure, magnetic and mechanical properties, J. Alloys Cmpd. **509S**, S155-S160 (2011).

[3] J. Gondro, J. Zbroszczyk, W. Ciurzyńska, J. Olszewski, M. Nabiałek, K. Sobczyk, J. Świerczek, A. Łukiewska, Structure and soft magnetic properties of bulk amorphous $(Fe_{0.61}Co_{0.10}Zr_{0.025}W_{0.02}Hf_{0.025}Ti_{0.02}B_{0.20})_{96}Y_4$ alloy, Archives of Metallurgy and Materials **55**(1), 85-90 (2010).

[4] J. Olszewski, J. Zbroszczyk, K. Sobczyk, W. Ciurzyńska, P. Bragiel, M. Nabiałek, J. Świerczek, M. Hasiak, A. Łukiewska, Thermal stability and crystallization of iron and cobalt – Based bulk amorphous alloys, Acta Physica Polonica A **114**(6), 1659-1666 (2008).

[5] K. Sobczyk, J. Zbroszczyk, M. Nabiałek, J. Olszewski, P. Bragiel, J. Świerczek, W. Ciurzyńska, A. Łukiewska, M. Lubas, M. Szota, Microstructure, magnetic properties and crystalization behaviour of bulk amorphous $Fe_{61}Co_{10}Zr_{2.5}Hf_{2.5}Ni_2W_{21}B_{20}$ alloy, Archives of Metallurgy and Materials **53**(3), 855-860 (2008).

[6] M. Nabialek, M. Dospial, M. Szota, P. Pietrusiewicz, J. Jedryka, Investigation of the Thermal and Magnetic Properties of $Fe_{61}Co_{10}Zr_{2.5}Hf_{2.5}Me_2W_2B_{20}$ (Me = Y, Nb, W, Ti, Mo, Ni) Bulk Amorphous Alloys Obtained by an Induction Suction Metod, J. Alloys Cmpd. **509**, 3382-3386 (2011).

[7] Z.P. Liu, C.T. Liu, J. Mater. Sci. **39**, 3965 (2004).

[8] B. Yang, C.T. Liu, T.G. Nieh, M.L. Morrison, P.K. Liaw, R.A. Buchanan, J. Mater. Res. **21**, 915-23 (2006).

[9] A. Inoue, Acta Mater **48**, 279-306 (2000).

[10] W.H. Wang, M.X. Pan, D.Q. Zhao, Y. Hu, H.Y. Bai, J Phys Condens Matter **16**, 3719-23 (2004).

[11] H. Kronmüller, Micromagnetism and microstructure of amorphous alloys, J. Appl. Phys. **52**, 1859-1864 (1981).

[12] H. Kronmüller, Micromagnetism in Amorphous Alloys, IEEE Trans. Magn. **15** 1218-1225 (1979).

[13] N. Lenge, H. Kronmüller, Low Temperature Magnetization of Sputtered Amorphous Fe-Ni-B Films, Phys. Stat. sol. (a) **95**, 621-633 (1986).

[14] M. Vazqeuez, W. Fernengel, H. Kronmüller, Approach to Magnetic Saturation in Rapidly Quenched Amorphous Alloys, phys. Stat. sol. (a) **115**, 547-553 (1989).

[15] T. Holstein, H. Primakoff, Magnetization Near Saturation in Polycrystalline Ferromagnets, Phys. Rev. **59**, 388-394 (1941).

[16] O. Kohmoto, High-field magnetization curves of amorphous alloys, J. Appl. Phys. **53**, 7486-7490 (1982).

[17] F. Carmona, V. Madurga, M. Vázquez, Approach to magnetic saturation in $(Co_{0.95}Fe_{0.05})_{75}Si_{15}B_{10}$ amorphous alloy, J. of Magn. Magn. Mater. **62**, 68-70 (1986).

[18] A. Inoue, B. Shen, A. Takeuchi, Fabrication, properties and applications of bulk glassy alloys in late transition metal-based systems, Mater. Sci. Eng. **A441**, 18-25 (2006).

[19] M. Stoica, R. Li, A. Reza. Yavari, G. Vaughan, J. Eckert, N. Van Steenberge, D. Ruiz Romera, Thermal stability and magnetic properties of FeCoBSiNb bulk metallic glasses **504S**, S123-S128 (2010).

Received: 20 February 2013.